Pergamon

Int. J. Heat Mass Transfer. Vol. 39, No. 14, pp. 2947–2956, 1996

0017-9310/96 $15.00+0.00

0017-9310(95)00365-7

A heat transfer correlation for condensation inside horizontal smooth tubes using the population balance approach

M. S. CHITTI and N. K. ANAND†

Department of Mechanical Engineering, Texas A&M University, College Station, TX 77843-3123, U.S.A.

(*Received* 25 *July* 1995 *and in final form* 28 *September* 1995)

Abstract—Population balance model with homogeneous flow assumption is applied for forced convective condensation inside smooth horizontal tubes. The purpose of the paper is to examine the applicability of the homogeneous flow assumption for in-tube condensation although the common observation is that annular flow is physically more realistic [Soliman and Azer, *ASHRAE Trans.* 77(1), 210–224 (1971); Stoecker and DeGrush, Oak Ridge National Laboratory 81-7762/6 and 01 (1987); Taitel and Dukler, *A.I.Ch.E. J.* **22,** 47–55 (1976)]. Lin's model [Lin, Ph.D. Dissertation (1979)] is applied suitably for the smooth tube conditions. Differences between Lin's model [Lin, Ph.D. Dissertation (1979)] and the present approach are clearly stated in the text. A correlation for the local heat transfer coefficient is obtained involving fewer parameters but with an additional constant and is applicable for oil–refrigerant mixtures also. Experimental data over a wide range of mass flux rates and condensing temperatures are used in obtaining the correlation. The predicted values of local *Nu*, compared with the experimental data indicate that 90% of the predictions are within ±20% of the experimental data, with a mean deviation of 13.2%.

INTRODUCTION

It is an established fact that during internal boiling or condensation, the changes in flow regimes (in the flow direction) cause a variation in the heat transfer rates. Hence, it is desirable to predict the effect of different flow regimes on the local heat transfer coefficients. As it is difficult to develop pure theoretical models, empirical or semi-empirical models (using some of the experimental data) were developed. Most of the semi-empirical models are based on either the Homogeneous Flow or the Separated Flow assumption. For condensation, the separated flow assumption is widely used as it is observed by several investigators that for high vapor velocities, annular flow is the predominant flow pattern, even for qualities as low as 25% [1–3]. In annular flow, the liquid attaches itself as a thin film along the circumference of the tube while the vapor core flows in the central region. But homogeneous flow assumption was also used by some investigators for condensation [4, 5], with a good degree of success. The reason being that the flow was modeled as a single phase fluid with some pseudo properties, varying along the flow direction according to the quality. The properties of this pseudo fluid were defined suitably as some mean values of the respective properties of liquid and gas phases. The literature survey reveals that very few authors [4–8] used the concept of population balance or the surface renewal theory. Of them, only Lin [5] used it to model both boiling and condensation heat transfer for refrigerant R-113 inside tubes with in-line static mixers. This was because the nature of the flow was well mixed (homogeneous) and highly agitated throughout the two-phase region due to the presence of the static mixers.

The objective of the current study is to examine for smooth tubes, the applicability of the homogeneous flow assumption using the population balance concept for condensation. This is done by suitably applying the population balance model used by Lin [5] to the smooth tube conditions, inspite of the common observation that annular flow is the predominant flow regime for condensation. A correlation is developed for local heat transfer coefficients, using the data for both pure and oil–refrigerant mixtures obtained in the current study. Experimental data for a wide range of mass flux rates and condensing temperatures are used in obtaining the correlation.

POPULATION BALANCE MODEL

The physical model of the problem is shown in Fig. 1 and the following simplifying assumptions are made in the analysis.

1. The flow pattern in the condenser is assumed to be homogeneous with liquid and vapor phases well mixed and highly agitated throughout the cross-section of the tube.

† Author to whom correspondence should be addressed.

NOMENCLATURE

A	area [m^2 (ft^2)]
C_p	specific heat at constant pressure [J kg^{-1} K^{-1} (Btu lbm^{-1} $°F^{-1}$)]
D	inner diameter of refrigerant tube [m (ft)]
e	error in the heat transfer coefficient
G	liquid refrigerant mass flux rate [kg m^{-2} s^{-1} (lbm h^{-1} ft^{-2})]
h	convective heat transfer coefficient [W m^{-2} K^{-1} (Btu h^{-1} ft^{-2} $°F^{-1}$)]
h_{fg}	latent heat of condensation [J kg^{-1} (Btu lbm^{-1})]
Δh	enthalpy change [J kg^{-1} (Btu lbm^{-1})]
k	thermal conductivity [W m^{-1} K^{-1} (Btu h^{-1} ft^{-1} $°F^{-1}$)]
L	length [m (ft)]
$\dot{M}$	mass flow rate [kg s^{-1} (lbm h^{-1})]
Pr	Prandtl number
q	mean heat flux in equation (10) [W m^{-2} (Btu h^{-1} ft^{-2})]
q_i	instantaneous heat flux in equation (9) [W m^{-2} (Btu h^{-1} ft^{-2})]
Q	heat transferred [W(Btu h^{-1})]
Re	Reynolds number
T	temperature [°C or K (°F)]
u	velocity [m s^{-1} (ft h^{-1})]
x	quality at any location z
y	distance from the tube wall [m (ft)]
z	axial location [m (ft)].

Subscripts

ave	average
b	bulk
calc	calculated
exp	experimental
i	inside of refrigerant tube
l	liquid condensate
m	mean value for any property of liquid–vapor bubble packet
o	evaluated at the tube wall surface
ref	refrigerant
sen	sensible
surf	surface
v	vapor
w	wall surface.

Greek symbols

α	thermal diffusivity [m^2 s^{-1} (ft^2 h^{-1})]
δ	distance [m (ft)]
μ	dynamic viscosity [kg m^{-1} s^{-1} (lbm h^{-1} ft^{-1})]
ρ	density [kg m^{-3} (lbm ft^{-3})]
θ	time [s].

2. As shown in Fig. 1, a small mass of liquid–vapor bubble packet which is initially at the bulk temperature T_b is assumed to come in contact with the cold tube surface at the temperature T_w.
3. The liquid–vapor packet is supposed to possess properties of some mean values of the liquid and vapor phases [equations (28)–(32)].
4. This liquid–vapor bubble packet is assumed to exchange heat with the tube surface in the contact time and is replaced by a similar packet from the main stream of the flow.
5. Such a heat transfer mechanism is assumed to be present throughout the condensing region and the mean residence time, i.e. the duration of the liquid–vapor bubble mixture in the condenser tube ($\bar{t}$) is obtained by integrating a suitable distribution function of their population (ϕ) as shown later.

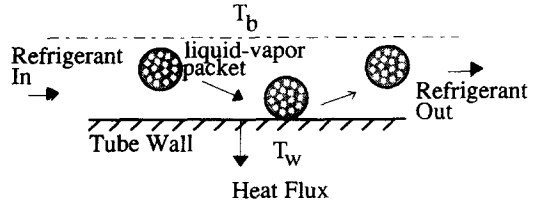

Fig. 1. Physical model for the population balance concept.

The expressions for the distribution function and the mean residence time of the liquid–vapor bubble packets are given in equations (1) and (2), respectively and their derivation can be seen in Fan *et al.* [4].

Heat transfer

We have from the population balance concept [5], the expressions for the distribution function and the mean residence time of the liquid–vapor bubble packets as

$$\bar{\phi}(\theta) = \frac{1}{\bar{\tau}} e^{-(\theta/\bar{\tau})} \tag{1}$$

and

$$s = \frac{1}{\bar{\tau}} = C_1 \frac{1}{\bar{t}} \tag{2}$$

where s is the frequency of the renewal of the liquid–vapor bubble packets which is inversely proportional to the mean contact time ($\bar{\tau}$) or mean residence time ($\bar{t}$) of the packets and C_1 is the constant of proportionality. The distribution function in equation (1) was originally proposed by Hsu and Graham [9] and used by Lin [5]. Equation (2) was initially proposed by Lin [5] in a different form with another term in the

numerator (2^N) accounting for N static in-line mixers. In this study it is applied to suit the smooth tube conditions without any static mixers ($N = 0$).

It should be noted that the mean contact time ($\bar{\tau}$) is the average time interval for which a liquid–vapor bubble packet is in contact with the condensing wall surface. On the other hand, the mean residence time ($\bar{t}$) is the average time for which a liquid–vapor bubble packet traverses in the total length of the condenser tube during the condensation process. It is logical to assume that both are directly proportional to each other.

Referring to Fig. 1, assuming that heat is lost by a liquid–vapor bubble packet to the tube surface during the time of contact by conduction, the governing equation is given by

$$\frac{\partial T}{\partial \theta} = \alpha_m \frac{\partial^2 T}{\partial y^2} \tag{3}$$

where

$$\alpha_m = \frac{k_m}{\rho_m C_{pm}} \tag{4}$$

and y is the distance from the tube surface and the mean properties are defined suitably to allow their variation with the local quality. Beyond a distance δ' from the tube surface, the temperature of the liquid–vapor bubble packet can be treated to be the same as the bulk temperature T_b. This distance is of the order of the size of the liquid–vapor bubble packets. Then the initial and boundary conditions can be written as

$$T = T_b \quad \theta = 0 \quad y > 0 \tag{5}$$

$$T = T_w \quad \theta > 0 \quad y = 0 \tag{6}$$

$$T = T_b \quad \theta > 0 \quad y > \delta'. \tag{7}$$

Equation (4) with the conditions in equations (5)–(7) can be solved for the temperature profile to obtain

$$\frac{(T-T_b)}{(T_w-T_b)} = \left[1 - \frac{y}{\delta'} - \frac{2}{\pi}\sum_{n=1}^{\infty}\left(\frac{1}{n}\sin\left(\frac{n\pi y}{\delta'}\right)e^{-(\pi^2 n^2 \alpha_m \theta/\delta'^2)}\right)\right]. \tag{8}$$

If $q_i(\theta)$ is the instantaneous heat flux at the wall in a contact time θ, then

$$q_i(\theta) = -k_m \left.\frac{\partial T}{\partial y}\right|_{y=0}. \tag{9}$$

Then the mean heat flux q is given by

$$q = \int_0^{\infty} q_i(\theta)\bar{\varphi}(\theta)\,d\theta. \tag{10}$$

Substituting for the temperature profile from equation (8) into equation (9), and the result in turn substituted into equation (10) leads to an expression for the mean heat flux across a unit area of the heat transfer surface given by

$$q = (T_w - T_b)\sqrt{\left(\frac{1}{\bar{\tau}} k_m \rho_m C_{pm}\right)}\coth\sqrt{\left(\frac{1}{\bar{\tau}}\frac{\delta'^2}{\alpha_m}\right)} \tag{11}$$

and from the definition of the inside heat transfer coefficient (h_i), h_i is obtained from equation (11) as

$$h_i = \frac{q}{(T_w - T_b)} = \sqrt{\left(\frac{1}{\bar{\tau}} k_m \rho_m C_{pm}\right)}\coth\sqrt{\left(\frac{1}{\bar{\tau}}\frac{\delta'^2}{\alpha_m}\right)}. \tag{12}$$

Since, for sufficiently large δ', $1/\bar{\tau}$, or $1/\alpha_m$

$$\coth\sqrt{\left(\frac{1}{\bar{\tau}}\frac{\delta'^2}{\alpha_m}\right)} \approx 1 \tag{13}$$

equation (12) can be further reduced to the following equation (14) whose derivation can also be obtained from Fan *et al.* [4] by applying to the present situation (no static mixer, $\Rightarrow N = 0$).

$$h_i = \sqrt{\left(\frac{k_m \rho_m C_{pm}}{\bar{\tau}}\right)} = (C_1)^{1/2}\sqrt{\left(\frac{k_m \rho_m C_{pm}}{\bar{t}}\right)}. \tag{14}$$

It can be seen that the mean residence time $\bar{t}$ is the main variable to be determined.

Mean residence time $\bar{t}$

The mean residence time $\bar{t}$ is derived in terms of the known parameters such as mean velocity (u_m) and tube length (L). Thus it can be shown that

$$\bar{t} = C_2 \frac{L}{u_m} \tag{15}$$

where C_2 is a constant of proportionality. In the current study, the mean velocity (u_m) is found from the mass balance as

$$u_m = C_3 \frac{\dot{M}}{A_l \rho_m} \tag{16}$$

where C_3 is a proportionality constant and A_l is the area occupied by the liquid condensate at a given cross-section. It is reasonable to use A_l since the mean velocity (u_m) decreases with an increase in the area of the liquid condensate as more of the liquid condenses in the flow direction. This is the simplest way to find the mean velocity. But Lin [5] assumed that u_m is approximately the same as the mean velocity of the liquid condensate. This mean velocity of the liquid condensate was found from the volumetric flow rate which in turn depends on the mass flow rate and the density. Also his assumption was based on the argument that the static mixers cause vigorous mixing of the liquid and vapor and hence the mean velocities of the two phases are of the same order. But in the experiments of the current study conducted by Chitti

[10] for smooth tubes, it is observed that the flow is predominantly annular flow for most of the condensation. Hence an assumption similar to Lin [5] is avoided in the current model development. Further, it is to be noted that u_m is varying and it is not constant along the flow direction since both A_l and the mean density (ρ_m) vary according to the local quality.

The area of the liquid condensate at any location can be obtained by

$$A_l = C_4 \delta'_{ave} D \tag{17}$$

where δ'_{ave} is an average size of the liquid–vapor bubble packets (characteristic dimension of the tube). Substituting equation (17) in equation (16) gives

$$u_m = \frac{C_3}{C_4} \frac{\dot{M}}{(\delta'_{ave} D)\rho_m}. \tag{18}$$

The quantity δ'_{ave} can be obtained from the Fourier's law of heat conduction occurring in the region near the wall within the distance δ'_{ave}. From an energy balance at the wall surface ($y = 0$), the following equation can be obtained as

$$Q_{tot} = -k_m A_{surf} \left.\frac{\partial T}{\partial y}\right|_{y=0} = -\dot{M}[(x_2 - x_1)h_{fg} + \Delta h_{sen}] \tag{19}$$

where A_{surf} is the heat transfer area of the surface given by

$$A_{surf} = \pi D L. \tag{20}$$

The term $(x_2 - x_1)$ is the change in the quality of the condensing fluid in a length L of the condenser tube. The quantity Δh_{sen} exists only at where the fluid is in a superheated or subcooled condition such as inlet of the test section in the experiments of the current study. Using equation (20) and approximating the derivative in equation (19) by $(T_b - T_w)/\delta'_{ave}$, equation (19) reduces to

$$\delta'_{ave} = C_5 \frac{-k_m(\pi D L)(T_b - T_w)}{-\dot{M}[(x_2 - x_1)h_{fg} + \Delta h_{sen}]}. \tag{21}$$

Substituting equation (21) in equation (18) for δ'_{ave}, the mean velocity is obtained as

$$u_m = \frac{C_3}{C_4 C_5} \frac{\dot{M}}{\left(\dfrac{-k_m(\pi D L)(T_b - T_w)}{-\dot{M}[(x_2 - x_1)h_{fg} + \Delta h_{sen}]}\right) D \rho_m}. \tag{22}$$

Substituting equation (22) in equation (15) and solving for $\bar{t}$ gives

$$\bar{t} = \frac{C_2 C_4 C_5}{C_3} \frac{k_m \rho_m (\pi D^2 L^2)(T_b - T_w)}{\dot{M}^2[(x_2 - x_1)h_{fg} + \Delta h_{sen}]}. \tag{23}$$

Substituting equation (23) in equation (14) and solving for h_i results in

$$h_i = (C_1)^{1/2} \sqrt{\left[\frac{k_m \rho_m C_{pm}}{\dfrac{C_2 C_4 C_5}{C_3} \dfrac{k_m \rho_m (\pi D^2 L^2)(T_b - T_w)}{\dot{M}^2[(x_2 - x_1)h_{fg} + \Delta h_{sen}]}}\right]}. \tag{24}$$

Combining all the proportionality constants into one constant C, equation (24) further reduces to

$$h_i = C\left[\frac{C_{pm}\dot{M}^2[(x_2 - x_1)h_{fg} + \Delta h_{sen}]}{\pi D^2 L^2 (T_b - T_w)}\right]^{1/2}. \tag{25}$$

Equation (25) in a non-dimensionalized form can be written as

$$\left[\frac{h_i D}{k_m}\right] = C\left[\left(\frac{C_{pm}^2 \mu_m^2}{k_m^2}\right)\left(\frac{\dot{M}^2}{\mu_m^2 D^2}\right)\left(\frac{D^2}{L^2}\right) \times \frac{[(x_2 - x_1)h_{fg} + \Delta h_{sen}]}{C_{pm}(T_b - T_w)}\right]^{1/2}. \tag{26}$$

The equation in terms of the non-dimensionalized numbers can be written as

$$[Nu] = C[Pr_m][Re_m]\left[\frac{D}{L}\right]\left[\frac{[(x_2 - x_1)h_{fg} + \Delta h_{sen}]}{C_{pm}(T_b - T_w)}\right]^{1/2}. \tag{27}$$

As can be seen from equation (27), all the quantities such as Pr_m and Re_m are defined uniformly in terms of the mean properties which is easier to use. But Lin [5] defined some quantities based on liquid and some others based on mean values. Also, since the mean velocity u_m was evaluated in terms of the volumetric flow rate of the liquid which required the liquid density, his final correlation consists of two more parameters. These are the ratios of the mean density and viscosity of the liquid condensate to those of the liquid–vapor bubble packet, respectively. Hence the current model requires less parameters and hence is simpler to use. The properties of the homogeneous liquid–vapor bubble packet based on mean quality [equation (28)] can be defined as

$$x_m = \frac{x_2 + x_1}{2} \tag{28}$$

$$\frac{1}{\rho_m} = \frac{x_m}{\rho_v} + \frac{(1 - x_m)}{\rho_l} \tag{29}$$

$$C_{p,m} = C_{p,v} x_m + C_{p,l}(1 - x_m). \tag{30}$$

The mean quantities of viscosity (μ_m) and thermal conductivity (k_m) also are evaluated using the above equation (30) by replacing the variable C_p with the desired variable. It is to be noted that for oil–refrigerant mixtures, the liquid phase viscosity is found from an equation similar to equation (29) as recommended by Chitti [10]. Referring to equation (29), it can be obtained by replacing ρ_m with μ_m (oil–refrigerant mixture), x_m with oil mass fraction, ρ_v with μ_{oil} and ρ_l with

μ_{ref}. For the viscosity of the mixture in the vapor phase, the data for oil was not available and hence it is assumed that oil does not effect the vapor phase oil–refrigerant mixture viscosity. The terms Pr_m and Re_m are defined in usual terms as

$$Pr_m = \frac{\mu_m C_{p,m}}{k_m} \tag{31}$$

$$Re_m = \frac{\dot{M}}{D\mu_m}. \tag{32}$$

EXPERIMENTS

A two-phase loop was built for conducting the condensation experiments. Tests were conducted for pure R-22, pure R32+R125 azeotropic mixture, oil (2.6% by mass) and R32+R125 mixture, and oil (5.37% by mass) and R32+R125 mixture for a wide range of mass flux rates and condensing temperatures. Details of the test apparatus are given in Chitti [10], and Chitti and Anand [11]. Hence, to avoid repetition, only a schematic of the test loop and the thermodynamic path of the refrigerant is given in Fig. 2. The details of the test procedure and the range of testing conditions can be obtained from Chitti [10]. For evaluating the heat transfer coefficient at a location, the local measurements in the neighboring points are used and this distance is taken as the length of the heat exchanger. Hence, the calculated values are in reality locally (regionally) averaged heat transfer coefficients. It was observed from the results that the mass flux rate was the dominant parameter affecting the local heat transfer coefficient while condensing temperature was found to have an insignificant effect in the range

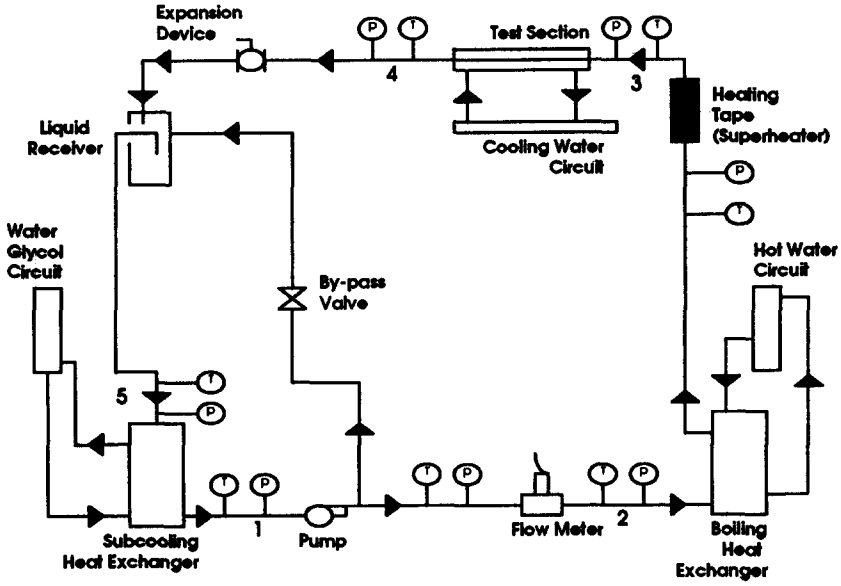

(a) Schematic of the Test Apparatus

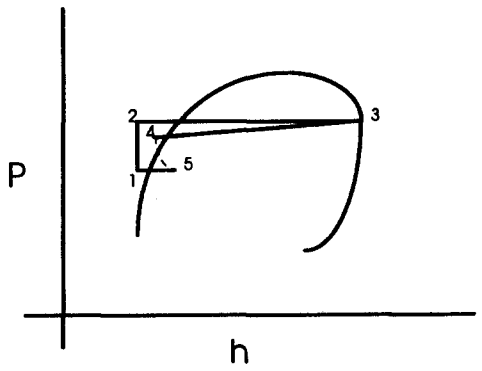

(b) Thermodynamic Path of the Refrigerant

Fig. 2. Schematic of the test apparatus and thermodynamic path of the refrigerant.

Table 1. Correlation results obtained from the current experimental data using the population balance concept

Parameter	Refrigerant Pure R-22	Refrigerant Pure R32+R125	Refrigerant Oil (2.6%) and R32+R125	Refrigerant Oil (5.37%) and R32+R125	Overall
No. of data points	83	177	81	81	422
Slope (C)	1.748533	1.711389	1.618496	1.394814	1.586100
Const. (b)	−124.52	−163.66	−100.02	−64.01	−102.68
SEE	101.5	80.3	64.5	87.7	94.2
COD	0.899	0.948	0.967	0.933	0.926
Min. % error	0.2	0.1	0.2	0.1	0.01
Max. % error	57.7	176.3	72.3	30.8	82.8
Average error (%)	16.4	12.1	13.1	10.3	13.2

of test conditions examined. The experimental data was compared in Chitti [10], and Chitti and Anand [11] with correlations of Akers *et al.* [12], Boyko and Kruzhilin [13], Shah [14], and Traviss *et al.* [15]. Of them, the data agreed well with Shah [14] and Traviss *et al.* [15] correlations to within 20% and 15%, respectively, and the reasons are explained in detail in Chitti and Anand [11]. Since the current model and the experimental data are in reasonably good agreement, it is assumed that the model agrees similarly with the correlations as well. A detailed uncertainty analysis was performed for the experimental data for which the recent guidelines proposed by Kim *et al.* [16] were followed although the basic methodology of Kline and McClintock [17] was adopted. From the analysis, it was found that the average uncertainty in the measurement of the heat transfer coefficients was ±25%.

RESULTS AND DISCUSSION

The coefficient C in equation (27) is obtained by fitting a straight line of the form $Nu = C\beta + b$, to a set of experimental data points using the method of least squares. Here, β is the coefficient of C on the right-hand side of equation (27). In all, 422 data points are used from the 141 test runs conducted for the four sets (substances) mentioned earlier. The value of C is obtained as 1.5861 with a correlation coefficient of 96.3% and a standard error of estimate of 94.2.

It should be noted that the regression lines in Table 1 have non-zero intercepts (or constant b). This indicates that the correlation is not valid for all values of $\dot{M} \geqslant 0$. However, it is valid in the range of the mass flux rates considered in this study, i.e. 150–500 kg m^{-2} s^{-1} (1.0–3.6 × 10^5 lbm h^{-1} ft^{-2}). The constant b in Table 1 has to be used in combination with the slope C for evaluating the local Nu. Similarly, the coefficients are determined for each of the above mentioned sets of test runs separately.

For each of the correlation set of Table 1, the deviation in the local Nu value is calculated at every data point as follows:

$$e_{per} = \frac{|h_{exp} - h_{calc}|}{h_{exp}} \quad (33)$$

and the average error or the mean derivation e_{ave} is then calculated by

$$e_{ave} = \frac{1}{n}\left(\sum_{1}^{n} \frac{|h_{exp} - h_{calc}|}{h_{exp}}\right) \times 100 \quad (34)$$

where n is the number of data points at which local Nu is calculated.

Comparison of Nusselt number

Figures 3(a)–(d) show the comparison of predicted values of the local Nusselt number obtained by the population balance model with that of the experimental values based on mean thermal conductivity. Figures 3(a)–(d) show results for pure R-22, pure R32+R125 mixture, oil (2.6%) and R32+R125 mixture, and oil (5.37%) and R32+R125 mixture respectively.

For R-22 in Fig. 3(a), except for few data points, most of the predicted values are within ±20% of the experimental values. The average error (16.4%) in Table 1 also indicates that the model has good predicting capability. From the standard error of estimate (SEE = 101.5) and the average Nusselt number occurring for R-22 which is approximately 750 [Fig. 3(a)], it can be seen that the average error is between 15 and 20%. The SEE is analogous to the standard deviation which would give an estimate of the scatter of the data about the mean value. For pure R32+R125 mixture in Fig. 3(b), most of the data points lie very close to the experimental values with a uniform deviation throughout the range of the data. This also indicates that the average error (12%) is less than that for R-22 (16.4%). The SEE value (80.3) and the average Nusselt number (1000) also suggest a similar low average error of 8%. For both the cases of oil concentrations of 2.6 and 5.37% in Figs 3(c) and (d), more than 90% of the predictions are within ±10% of the experimental values. This shows that the model is valid for oil–refrigerant mixtures provided proper care is taken in evaluating the mixture properties, especially the viscosity. A detailed discussion on this property (viscosity) is given in Chitti [10].

Effect of mass flux rate on local h

Figure 4 shows a plot for changes in flow regimes occurring during condensation for pure R32+R125

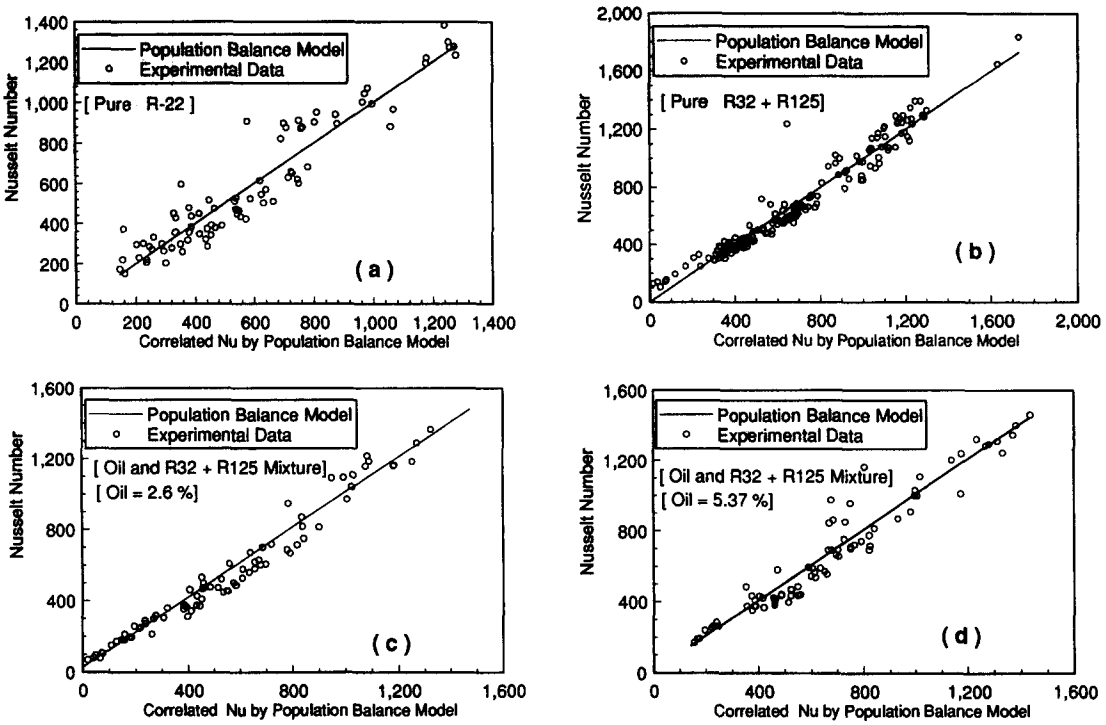

Fig. 3. Comparison of predicted local Nu by population balance model with experiments.

	Run	G kg/ sq.m s (lbm/hr sq.ft)	P(sat) kPa (psia)	T(sat) deg. C (deg. F)	Heat Bal. % error
—o—	1	207.5 (1.533 e5)	2,171 (315.1)	35.17 (95.3)	0.97
—◇—	2	311.6 (2.298 e5)	1,836 (266.4)	28.56 (83.4)	9.62
---△---	3	392.0 (2.891 e5)	2,360 (342.5)	38.56 (101.4)	1.90
— □—	4	490.5 (3.617 e5)	2,318 (336.4)	37.83 (100.1)	4.90

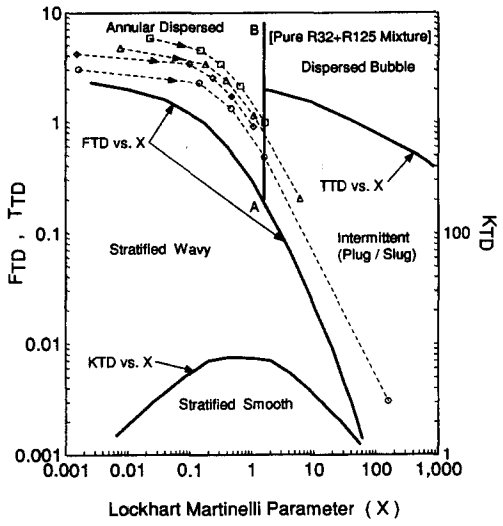

Fig. 4. Variation of the flow regimes during condensation of pure R32+R125 mixture at different mass flux rates (Taitel and Dukler [3]).

mixture. It is representative of similar graphs plotted by Chitti [10] for pure R-22, and two oil–refrigerant mixtures of 2.6 and 5.37% oil using the flow pattern map of Taitel and Dukler [3]. In other words, the trend of the curves regarding the flow regimes in Fig. 4 for R32+R125 mixture is valid for other sets of data (R-22 and oil–refrigerant mixtures) also. From this figure, it can be noted that mass flux rate is the predominant parameter influencing the flow regime while the condensing temperature has insignificant effect. Also most of the data points are in the annular flow regime except for the points near the transition line AB where the flow could be either slug/plug or bubbly flow (homogeneous). Interestingly, the predictions by the population balance model indicate that homogeneous flow assumption throughout the condenser tube is a reasonable one as explained below.

Figure 5 shows the variation of local h with the quality at different mass flux rates as predicted by the population balance model in comparison with the experimental data for R-22. The four test runs plotted are in the increasing order of the mass flux rate and represent the total range of the mass flux rates and condensing temperatures used in the study. Since the condensing temperature is found to have insignificant effect on the local h values, they are omitted from all the plots (Figs 5–8) in this paper. Arguing similarly, the plots are valid for same condensing temperature also. It can be observed from the Fig. 5 that the model underpredicts the experimental data for the lowest

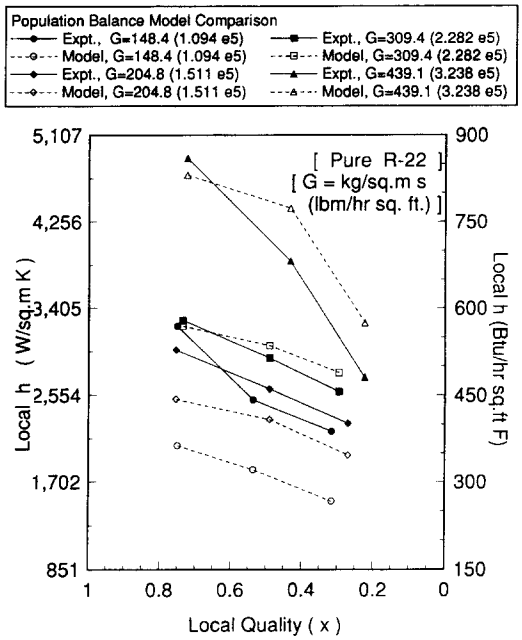

Fig. 5. Variation of the local h with quality by population balance model and experiments for pure R-22.

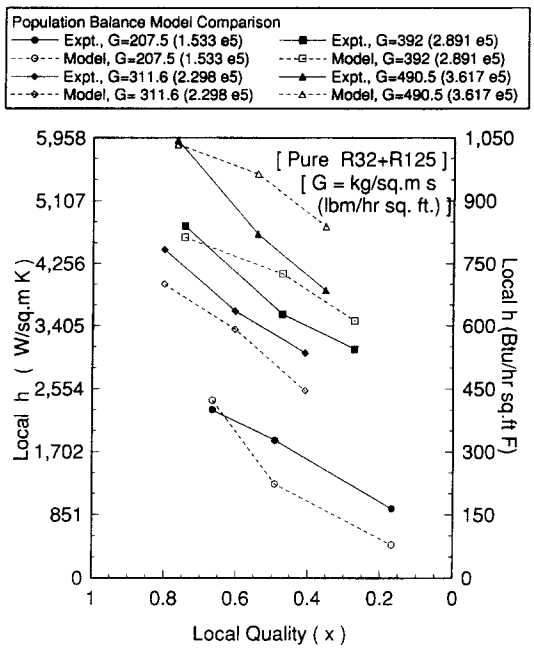

Fig. 6. Variation of the local h with quality by population balance model and experiments for pure R32+R125.

mass flux rate of 148 kg m^{-2} s^{-1} (1.094 lbm h^{-1} ft^{-2}). The reason for the higher experimental h values for this mass flux rate was discussed in detail in Chitti [10], and Chitti and Anand [11]. Also there was higher uncertainty in the flow sensor readings for this low mass flux rate from calibration in addition to the difficulty in obtaining the stable flow conditions. So actually the experimental values of local h could be lower than those shown in Fig. 5 for the low mass flux rate of 148 kg m^{-2} s^{-1} (1.094 lbm h^{-1} ft^{-2}). Taking into account these factors, the predictions can be considered reasonable. The above mentioned effects can be seen to be diminishing for higher mass flux rates plotted. However, the model tends to overpredict the experimental values by about 10% for mass flux rates greater than 350 kg m^{-2} s^{-1} (2.6×10^5 lbm h^{-1} ft^{-2}). This could be because of the fact that for these high mass flux rates, the flow would be predominantly in annular regime rather than homogeneous flow even for low qualities. Inspite of the population balance model being based on the homogeneous flow assumption, if the uncertainty in the experimental values is also taken into account, then the predictions can be said to be reasonably good.

Figures 6–8 show similar plots for the variation of predicted and experimental local h with quality for mass flux rate as the parameter for pure R32+R125 mixture, and two oil–refrigerant mixtures of 2.6 and 5.37%, respectively. It can be observed from Fig. 6 that for pure R32+R125 mixture, the model underpredicts the local h values. It is to be noted that the amount of deviation is the same for both R-22 (curve 2 with diamond symbol in Fig. 5) and pure R32+R125 mixture (curve 1 with circular symbol in Fig. 6) which have approximately the same mass flux rate of about 205 kg m^{-2} s^{-1} (1.52×10^5 lbm h^{-1} ft^{-2}). Also from Figs. 5–8, it can be observed that except in Fig. 8, the model begins to overpredict the experimental values

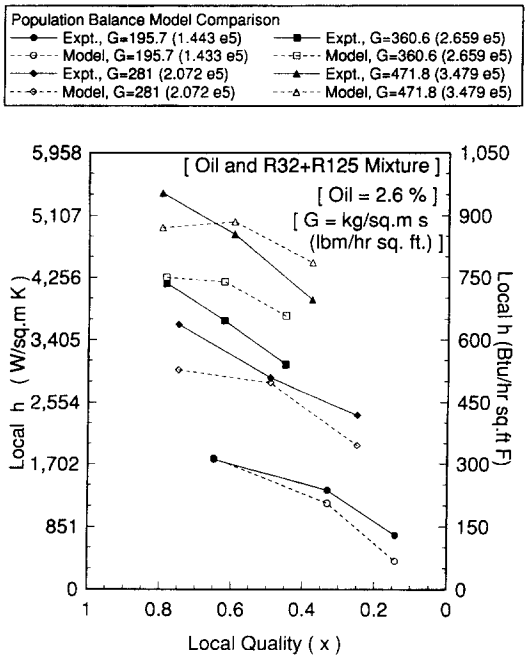

Fig. 7. Variation of the local h with quality by population balance model and experiments for oil (2.6%) and R32+R125 mixture.

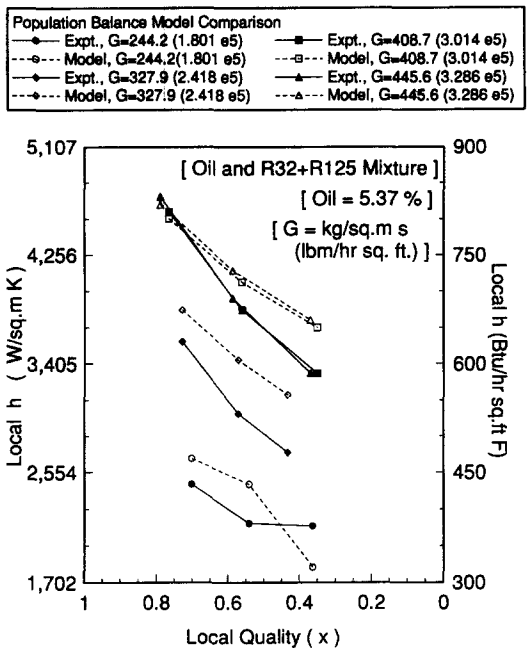

Fig. 8. Variation of the local h with quality by population balance model and experiments for oil (5.37%) and R32+R125 mixture.

of local h at approximately the mass flux rate of 340–350 kg m^{-2} s^{-1} (2.5–2.6 × 10^5 lbm h^{-1} ft^{-2}). Hence it can be inferred that the model is valid for the mass flux rates between 250 and 350 kg m^{-2} s^{-1} (1.8–2.6 × 10^5 lbm h^{-1} ft^{-2}). For mass flux rates lower and higher than this range, the model tends to under- and overpredict the local h values, respectively. Although the flow regime map (Fig. 4) suggests mostly annular flow pattern in this range of the mass flux rates and for qualities 0.3–0.7, the predictions seem to be reasonably good to within 10% of the experimental values. This can be observed inspite of the homogeneous flow assumption made in the model development. However, for mass flux rates higher than considered in this study, further tests have to be done in order to understand the trend of the predictions (i.e. if the degree of over prediction increases). Nevertheless, for most of the range of the parameters considered in this study, the average over- or underprediction is not more than 20%. Since the amount of the uncertainty in the experiments is also of the same order, it can be stated that the model predictions are reasonable. Hence the model can still be applied in the range of parameters studied with the above mentioned accuracy.

In summary, the comparison of the predictions of the current population balance model with the experimental results indicate that the model can be used to predict the local heat transfer coefficients within ±20%. This also suggests that population balance concept although is based on the homogeneous flow assumption, can still be applied for condensation inside smooth tubes, with reasonably good accuracy.

SUMMARY

Population balance concept is successfully applied to calculate the local heat transfer coefficients during two-phase forced convective condensation. The current model is a modified version of Fan *et al.* [4] and Lin [5] and used data for oil–refrigerant mixtures also. Although, it has fewer parameters in the final correlation equation than Fan *et al.* [4] and Lin [5], it has an additional constant. Also, the Reynolds and Prandtl numbers in the final correlation equation are defined uniformly based on the mean quantities [equation (27)]. Lin's model [5] is applied suitably here to suit smooth tube conditions since it was originally developed for tubes with in-line static mixers. The current model is applicable for oil–refrigerant mixtures also while Lin [5] has not tested his model for such mixtures. However, the current model is valid only for the mass flux rates tested in the current study unlike Lin's [5] model which is good even for $\dot{M} \geqslant 0$.

The results indicate that the predicted values for all the four sets of data (two pure refrigerants and two oil–refrigerant mixtures) agree well with the experimental data to within ±20%, with a mean deviation of 13.2%.

The current model is valid in the mass flux rate and quality ranges of 250–350 kg m^{-2} s^{-1} (1.8–2.6 × 10^5 lbm h^{-1} ft^{-2}) and 0.3–0.7, respectively. The model tends to under- and overpredict the experimental local h values by about 15% on an average for lower and higher mass flux rates, respectively.

Acknowledgements—This research, supported by the Texas Higher Education Coordinating Board under the Texas Advanced Technology Research Program (TARTP) (Project no. 32131-70640) and by the ASHRAE in the form of Graduate Student-in-Aid Fellowship are greatly acknowledged. Inputs of Drs D. L. O'Neal and L. Swanson of HTRI are greatly appreciated.

REFERENCES

1. M. Soliman and N. Z. Azer, Flow patterns during condensation inside a horizontal tube, *ASHRAE Trans.* 77(1), 210–224 (1971).
2. W. F. Stoecker and D. DeGrush, Measurements of heat-transfer coefficients of nonazeotropic refrigerant mixtures condensing inside horizontal tubes, Oak Ridge National Laboratory/Sub/81-7762/6 and 01 (1987).
3. Y. Taitel and A. E. Dukler, A model for predicting flow regime transitions in horizontal and near horizontal gas–liquid flow, *A.I.Ch.E. Jl* **22,** 47–55 (1976).
4. L. T. Fan, S. T. Lin and N. Z. Azer, Surface renewal model of condensation heat transfer in tubes with in-line static mixers, *Int. J. Heat Mass Transfer* **21,** 849–855 (1978).
5. S. T. Lin, Augmentation of two-phase heat transfer with in-line static mixers, Ph.D. Dissertation, Kansas State University, Manhattan, KS (1979).
6. L. Swanson and I. Catton, Surface renewal theory for turbulent mixed convection in vertical ducts, *Int. J. Heat Mass Transfer* **30**(11), 2271–2279 (1987).
7. E. B. Nauman, Residence time distribution theory for unsteady stirred tank reactors, *Chem. Engng Sci.* **24,** 1461 (1969).

8. M. S. K. Chen, The theory of micromixing for unsteady state flow reactors, *Chem. Engng Sci.* **26,** 17 (1971).
9. Y. Y. Hsu and R. W. Graham, *Transport Processes in Boiling and Two-Phase Systems*, pp. 13–14. McGraw-Hill, New York (1976).
10. M. S. Chitti, Condensation of a new alternative refrigerant inside smooth horizontal tubes, Ph.D. Dissertation, Texas A&M University, College Station, TX (1994).
11. M. S. Chitti and N. K. Anand, An analytical model for local heat transfer coefficients for forced convective condensation inside smooth horizontal tubes, *Int. J. Heat Mass Transfer* **38,** 615–627 (1995).
12. W. W. Akers, H. A. Deans and O. K. Crosser, Condensation heat transfer within horizontal tubes, *Chem. Engng Prog. Symp. Ser.* **55**(29), 171–176 (1959).
13. L. D. Boyko and G. N. Kruzhilin, Heat transfer and hydraulic resistance during condensation of steam in a horizontal tube and in a bundle of tubes, *Int. J. Heat Mass Transfer* **10,** 361–373 (1967).
14. M. M. Shah, Heat transfer during film condensation in tubes and annuli: a review of the literature, *ASHRAE Trans.* **87**(1), 1086–1105 (1981).
15. D. P. Traviss, W. M. Rohsenow and A. B. Baron, Forced-convection condensation inside tubes: a heat transfer equation for condenser design, *ASHRAE Trans.* **79**(1), 157–165 (1973).
16. J. H. Kim, T. W. Simon and R. Viskanta, *Journal of Heat Transfer* policy on reporting uncertainties in experimental measurements and results, Editorial, *ASME J. Heat Transfer* **115**(1), 5–6 (1993).
17. S. J. Kline and F. A. McClintock, Describing uncertainties in single-sample experiments, *Mech. Engng* **75,** 3–8 (1953).